nature communications

Article

https://doi.org/10.1038/s41467-024-50704-3

Spatial heterogeneity of extinction risk for flowering plants in China

Received: 18 August 2023

Accepted: 18 July 2024

Published online: 28 July 2024

Check for updates

Lina Zhao[1,2], Jinya Li[3], Russell L. Barrett[4,5], Bing Liu[1,2,6], Haihua Hu[1,2], Limin Lu[1,2] ✉ & Zhiduan Chen[1,2,6] ✉

Understanding the variability of extinction risk and its potential drivers across different spatial extents is crucial to revealing the underlying processes of biodiversity loss and sustainability. However, in countries with high climatic and topographic heterogeneity, studies on extinction risk are often challenged by complexities associated with extent effects. Here, using 2.02 million fine-grained distribution records and a phylogeny including 27,185 species, we find that the extinction risk of flowering plants in China is spatially concentrated in southwestern China. Our analyses suggest that spatial extinction risks of flowering plants in China may be caused by multiple drivers and are extent dependent. Vegetation structure based on proportion of growth forms is likely the dominant extinction driver at the national extent, followed by climatic and evolutionary drivers. Finer extent analyses indicate that the potential dominant extinction drivers vary across zones and vegetation regions. Despite regional heterogeneity, we detect a geographical continuity potential in extinction drivers, with variation in West China dominated by vegetation structure, South China by climate, and North China by evolution. Our findings highlight that identification of potential extent-dependent drivers of extinction risk is crucial for targeted conservation practice in countries like China.

Biodiversity loss is one of the most pressing environmental issues today[1,2]. Globally, at least 571 plant species are considered extinct in the wild since 1750, more than twice the combined number of birds, mammals, and amphibians[3]. About 34% of conifers, 69% of cycads, and 70% of evaluated flowering plant species are ranked as threatened by the International Union for Conservation of Nature (IUCN, https://www.iucnredlist.org/, accessed October, 2022). Limited understanding of extinction processes will seriously hinder efforts to reverse the trend of biodiversity loss by 2030 and impede the UN's Sustainable Development Goal 15 'life on land', as global change is driving a rapid increase in 'unpredictable' extinctions. Therefore, clarifying spatial patterns of extinction risk and their underlying drivers is crucial for developing effective strategies to safeguard, recover, and promote the sustainable use of terrestrial ecosystems, including halting biodiversity loss[1].

Extinction risk for plants has been considered to be spatially non-random and has geospatial selectivity[4,5], i.e., species with similar geographical distribution ranges tend to suffer similar extinction risks[6,7]. Numerous comparative studies have provided insights into why some species are more vulnerable than others, linking vulnerability to extinction with specific drivers[8]. Extrinsic environmental factors, such as climate change, topographic heterogeneity, and anthropogenic pressures have been shown to affect population size and distribution of species[8–10]. In particular, explosive human population growth and

[1]State Key Laboratory of Plant Diversity and Specialty Crops & Key Laboratory of Systematic and Evolutionary Botany, Institute of Botany, Chinese Academy of Sciences, 100093 Beijing, China. [2]China National Botanical Garden, 100093 Beijing, China. [3]State Key Laboratory of Urban and Regional Ecology, Research Center for Eco-Environmental Sciences, Chinese Academy of Sciences, 100085 Beijing, China. [4]National Herbarium of New South Wales, Australian Botanic Garden, Locked Bag 6002, Mount Annan 2567 NSW, Australia. [5]Evolution and Ecology Research Centre, School of Biological, Earth, and Environmental Sciences, University of New South Wales, Kensington 2052 NSW, Australia. [6]Sino-Africa Joint Research Center, Chinese Academy of Sciences, Wuhan 430074, China. ✉e-mail: liminlu@ibcas.ac.cn; zhiduan@ibcas.ac.cn

anthropogenic environmental deterioration since the second half of the 20th century have led to significant biodiversity loss and ecosystem imbalance[2,11]. Recent studies suggest that vegetation structure (e.g., proportion of growth forms) and evolutionary dynamics (e.g., divergence time, diversification rate, and weighted evolutionary distinctiveness) also play crucial roles in determining threat status[4,12–15]. However, very few investigations have comprehensively incorporated these drivers, especially the evolutionary factors, in the assessment of extinction risks at large extents[7,12] (see Fig. 1 and Supplementary Data 1 for more details on hypotheses of extinction drivers).

Previous studies across large spatial and taxonomic levels have demonstrated that threatening processes, such as specific climatic factors related to extinction risk, are scale or extent dependent[11,16]. For countries with high climatic and topographic heterogeneity, analysis of drivers of threatening processes has usually proven unreliable or of low predictability when treating the region as a whole[16,17]. This is because the stability of species' populations is closely linked to drivers at a local scale or extent, due to regional or small-extent environmental heterogeneity[16]. Recognizing the indispensable role of spatial scale and/or extent effects is therefore critical in the assessment of extinction risks[17] (See Supplementary Note 1 for comparison between scale and extent effects). To address this, when applied to larger spatial extents or morphologically diverse groups of taxa, studies based on multivariate analyses and incorporating scale or extent effects are needed to fully understand the spatial characteristics of extinction risk and their underlying driving forces.

China possesses highly heterogeneous topography, diverse climatic conditions, and varied ecological environments, contributing to its exceptional biodiversity and designation as one of the world's 17 megadiverse countries (Fig. 2 and Supplementary Fig. 1). However, biodiversity in China is under threat, with a significant proportion of species at high risk of extinction[18]. According to the IUCN Red List criteria, ca. 11% of China's flowering plant species had been classified as threatened based on the assessments of Chinese higher plants in 2013 and 2020[18–20]. Revisions in the Red List Index reveal that the overall extinction risks for plants in China have not been alleviated[21]. Some studies suggest that threatened flowering plants in China are primarily affected by climate factors[22] or anthropogenic influence[23], or both[10,24], while others suggest that the underlying drivers may be more complex[25,26]. Each of these studies usually focused on single drivers[22,23], under-sampled specific plant clades[24], or high-level taxonomic groups[25]. Considering the heterogeneous topography and diverse vegetation associations in China, the spatial heterogeneity of extinction risk requires examination in more detail. Key questions that remain unanswered are, how uniform are the threatening processes affecting flowering plants in China at varying spatial extents, and what are the dominant spatial-dependent drivers? Even with comprehensive assessments of environmental and evolutionary drivers, the issue of extent must still be addressed.

In this work, we show that potential extinction drivers for flowering plants in China are regionally complex by integrating a 27,185-taxon phylogeny and 2.02 million fine-grained distribution records in comprehensive model-based analyses. Our objectives are (1) to clarify the spatial variability of extinction risk for flowering plants in China; and (2) to identify dominant drivers for flowering plant extictions across different spatial extents to understand the critical spatial differences in extinction risk.

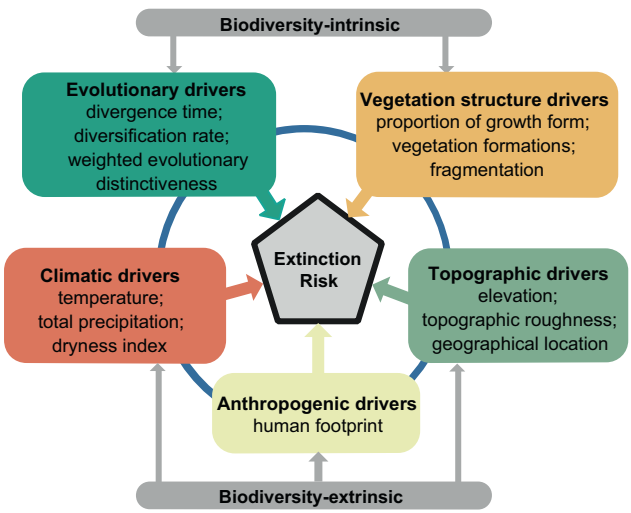

Fig. 1 | Main hypothesized extinction drivers for flowering plants in China. Potential extinction drivers of flowering plants in China were divided into two categories: biodiversity-intrinsic drivers and biodiversity-extrinsic drivers. The former includes evolutionary and vegetation structure drivers, while the latter includes climatic, topographic, and anthropogenic drivers.

Results

Spatial diversity patterns of extinction risk

We assessed the autocorrelation of diversity measures of flowering plants (i.e., threatened species richness, TR; the proportion of threatened species, propTR) and potential extinction drivers using Moran's *I*[27]. The patterns of TR and propTR were spatially similar ($r = 0.75$; $p < 0.001$), and both showed significant spatial concentration (Moran's $I \in (0.25, 0.49)$; $p < 0.001$) (Fig. 3a, b). Threatened species were spatially aggregated by latitude, longitude, and elevation (Fig. 3g–l). Notably, 80.9% of threatened species were concentrated in regions of 22–29°N (Figs. 3g), 81.0% in regions of 98–110°E (Figs. 3i), and 94.5% at elevations of 600–1800 m (Fig. 3k). More than 60% of threatened species were found at the intersection of the above concentrated regions, i.e., the junction of Tibet, Yunnan, and Sichuan provinces (Fig. 2).

Phylogenetic diversity (PD) of threatened flowering plants (Supplementary Fig. 2a) exhibited a spatial pattern similar to that of PD for all flowering plants in China (Fig. 3e). Notably, regions with high PD for threatened species were predominantly located in South China, contrasting with comparatively lower PD in West and North China (Supplementary Fig. 2a). According to the standardized effective size of PD (sesPD), threatened species were phylogentically clustered in West China, while it was phylogenetically overdispersed in selected regions of East and North China, suggesting that threatened species in West China were more closely related than expected, whereas those in East and North China were more distantly related (Supplementary Fig. 2b, c).

Phylogenetic signals of extinction risk

We divided China's landscape into eight vegetation regions and calculated Fritz's *D* values to examine the phylogenetic signals in discrete variables (threatened or not) for each vegetation region. We further compared the observed *D* values with simulated values under the Brownian motion and random models. Our analyses showed significant phylogenetic signals of extinction risk of flowering plants within each vegetation region ($D \in (0.681, 0.802)$, $p_0 < 0.01$, $p_1 < 0.01$; Fig. 4; Supplementary Data 2). Significantly heterogeneity has been observed for extinction risk across vegetation regions ($q = 0.65$, $p < 0.001$). Generally, the extinction risk was higher in the southern regions than in the north. The *Tropical monsoon rainforests* (V, see the codes in Fig. 2, hereafter) had the highest proportion of threatened species (propTR = 0.129; Fig. 4), while the *Cold temperate coniferous forests* (I) had the lowest (propTR = 0.020; Fig. 4).

We also divided China into three zones according to topography and climate types and calculated Fritz's *D* values to further detect phylogenetic signal of extinction risks at larger extents. We found that the extinction risk of flowering plants also showed a significant

https://doi.org/10.1038/s41467-024-50704-3

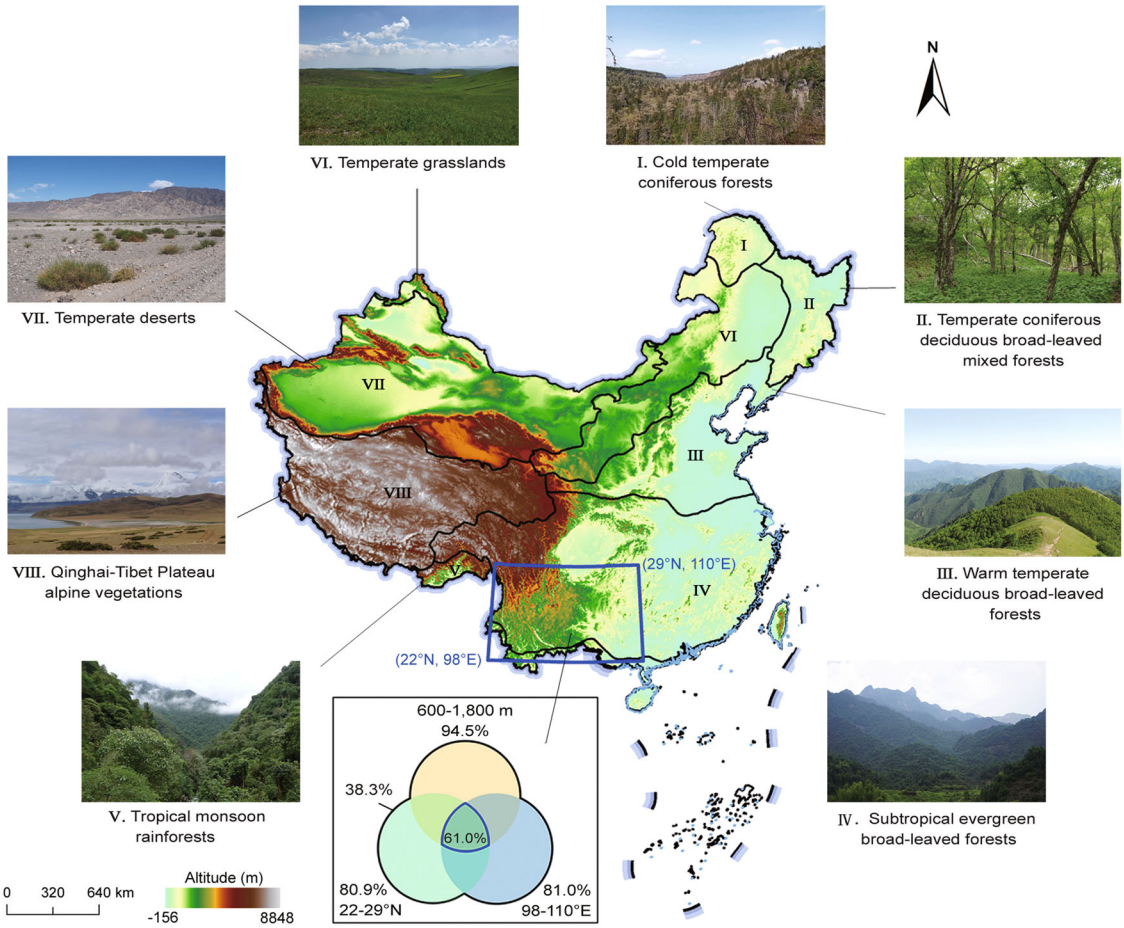

Fig. 2 | Topography and major vegetation regions in China, highlighting spatial concentration of threatened plants. Black lines on the map represent boundaries of vegetation regions based on the *Vegetation Regionalization Map of China*, with representative photos for each region shown around the map. The blue box on the map shows the spatial concentration of threatened plants in 22–29°N and 98–110°E. A Venn diagram shows the proportion of threatened species in three spatial dimensions, with different colored circles represent the spatial distribution of threatened species in 22–29°N (green), 98–110°E (blue), and 600–1800 m (yellow), respectively. All photographs published with permission from Dan Xie (I, VI), Bing Liu (II, III, V, VII), and Limin Lu (IV, VIII). The national boundary layer was downloaded from the Standard Map Service Website (Approval Number is GS(2019)1823; http://bzdt.ch.mnr.gov.cn/browse.html?picId=%224o28b0625501ad13015501ad2bfc0256%22, accessed October 2022).

phylogenetic signal within each zone ($D \in (0.709, 0.812)$, $p_0 < 0.001$, $p_1 < 0.001$; Fig. 5) and significant heterogeneity has also been observed for extinction risk across zones ($q = 0.58$, $p < 0.001$).

Drivers of extinction risk at national, regional, and zone extents

The values of Moran's *I* showed that all diversity measures (Moran's $I \in (0.16, 0.49)$; $p < 0.001$; Fig. 3a–f) and potential extinction drivers (Moran's $I \in (0.17, 0.69)$; $p < 0.001$; Supplementary Data 3) are spatially aggregated. These drivers involved a total of 24 variables (including six vegetation structure drivers), four evolutionary drivers, six climatic drivers, seven topographic drivers, and one anthropogenic driver in the initial partial least squares path model (plspm; see more details in 'Methods' section and Supplementary Dataset 1, 3). Different drivers showed varying correlations with the number of threatened species (TR, Supplementary Fig. 3) and the proportion of threatened species (propTR, Supplementary Fig. 4).

We utilized plspm to elucidate the potential pathways by which biodiversity-intrinsic and -extrinsic drivers have contributed to the extinction risks of flowering plants (i.e., extinction risks) in China and in different vegetation regions or zones, respectively. Three different levels of models, *national-plspm*, *regional-plspms*, and *zone-plspms*, were applied for spatial modeling. The combined effects of multiple drivers varied across plspms at national, regional, and zone levels, highlighting the need to understand all threatening processes applicable at different extents.

When China was treated as a single region, the final optimized *national-plspm* can account for 55.2% of the spatial extinction risk ($R^2 = 0.552$, GoF = 0.629; Supplementary Fig. 5; Supplementary Dataset 4–7). The primary model of *national-plspm* consisted of five types of extinction drivers (latent variables) and had sufficient explanatory power (R^2) for all latent variables ($R^2 \in (0.269, 0.708)$, Supplementary Data 4). Vegetation structures (i.e., the proportion of herbs) were identified as the dominant drivers at the national extent (negative effect standardized path coefficient, pcoef.std = −0.599, $p < 0.001$; Supplementary Data 6), under both the total effects (Supplementary Data 6) and direct effects (Supplementary Fig. 5). Climatic (positive effect; pcoef.std = 0.551, $p < 0.001$; i.e., precipitation, Prec) and evolutionary (positive effect; pcoef.std = 0.499, $p < 0.001$; i.e., median weighted evolutionary distinctiveness, medianWED) drivers also influenced extinction risks of flowering plants in China (Supplementary Data 6).

The *regional-plspm*s were created to deconstruct the spatial influence of extinction risks for different vegetation regions. All *regional-plspms* fit very well, and their GoF values mostly meet the requirement (GoF $\in$ (0.369, 0.622); Fig. 6). Overall, except for $plspm_{VI}$ and $plspm_{VII}$, most *regional-plspms* can explain 25.2–53.3% of

https://doi.org/10.1038/s41467-024-50704-3

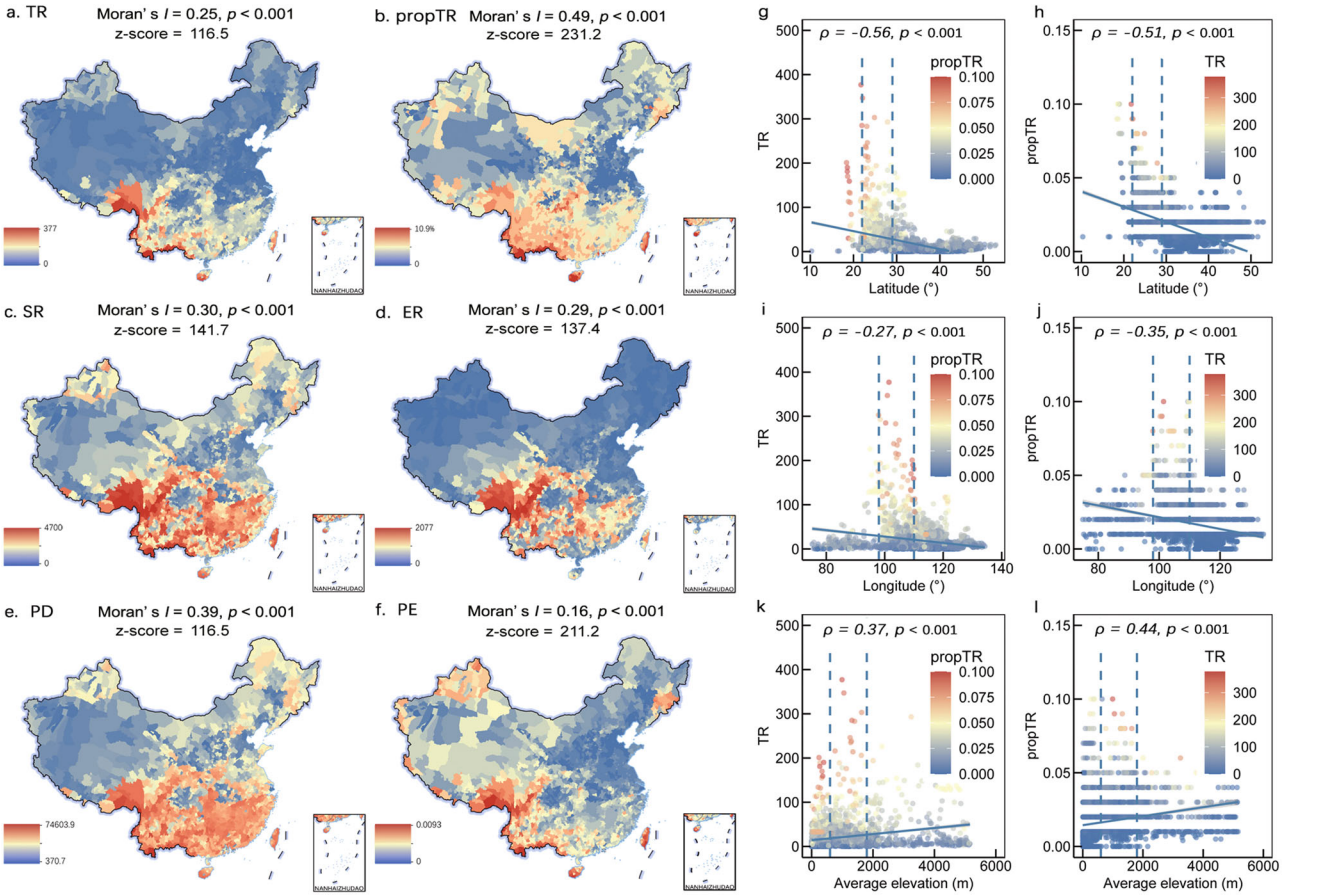

Fig. 3 | Spatial distribution patterns of different diversity measures for flowering plants in China. The diversity measures are threatened species richness (TR, **a**), proportion of threatened species (propTR, **b**), species richness (SR, **c**), endemic species richness (ER, **d**), phylogenetic diversity (PD, **e**), and phylogenetic endemism (PE, **f**), respectively. The significance level of the degree of spatial clustering for different diversity measures are listed after each Moran's *I*. Pointplots on the right are latitudinal (**g**, **h**), longitudinal (**i**, **j**), and altitudinal patterns (**k**, **l**) of TR and propTR, respectively, with the colored bars representing values of propTR (**g**, **i**, **k**) and TR (**h**, **j**, **l**) in counties ($n = 2894$ counties). Points between two dotted lines in each pointplot are the core latitudinal (**g**, **h**), longitudinal (**i**, **j**), and altitudinal (**k**, **l**) regions of TR and propTR, respectively. ρ is the correlation coefficient between different measures. Colors from blue to red reflect values of different diversity measures from low to high. The national boundary layer was downloaded from the Standard Map Service Website (Approval Number is GS(2019)1823; http://bzdt.ch.mnr.gov.cn/browse.html?picId=%224o28b0625501ad13015501ad2bfc0256%22, accessed October 2022).

extinction risks of flowering plants at the regional level (Fig. 6 and Supplementary Dataset 8–11). While the extinction drivers varied across vegetation regions, some adjacent regions shared similar dominant drivers: vegetation structure drivers for *Temperate deserts* (VII; positive effect; pcoef.std = 0.324, $p < 0.001$) and *Qinghai-Tibet Plateau alpine vegetations* (VIII; positive effect; pcoef.std = 0.612, $p < 0.001$), evolutionary drivers for *Temperate coniferous deciduous broad-leaved mixed forests* (II; positive effect; pcoef.std = 0.484, $p < 0.001$), *Warm temperate deciduous broad-leaved forests* (III; negative effect; pcoef.std = −0.434, $p < 0.001$), and *Temperate grasslands* (VI; negative effect; pcoef.std = −0.195, $p < 0.001$), and climatic drivers for *Subtropical evergreen broad-leaved forests* (IV; positive effect; pcoef.std = 0.687, $p < 0.001$) and *Tropical monsoon rainforests* (V; positive effect; pcoef.std = 0.755, $p < 0.001$) (Fig. 6; Supplementary Data 11).

Dominant extinction drivers based on the well-fitted *zone-plspms* (GoF∈ (0.438, 0.619), R^2∈ (0.139, 0.543); Fig. 5) were consistent with those revealed by the *regional-plspms*, with vegetation structure drivers dominanting West China (including vegetations VII and VIII; negative effect; pcoef.std = −0.239, $p < 0.001$), evolutionary drivers dominanting North China (including vegetations II, III and VI; positive effect; pcoef.std = 0.431, $p < 0.001$), and climatic drivers dominanting South China (including vegetations IV and V; positive effect; pcoef.std = 0.869, $p < 0.001$) (Fig. 5; Supplementary Dataset 12–15), further supporting spatial heterogeneity of extinction risk for flowering plants across China.

Discussion

Using a species-level phylogeny and fine-grained county-level distribution records, we find that threatened flowering plants are significantly geospatially aggregated, and the core regions are located between 22–29°N, 98–110°E, and 600–1800 m elevation (Figs. 2, 3). Spatial concentration of high extinction risk areas are in the Nyainqêntanglha Mts (36), Boshula Mts (38), Gaoligong Mts (39), Tanitantaweng Mts (40), Nushan Mts (41), Yunling Mts (42) and Shaluli Mts (43), as well as in West Sichuan, including the Daxue Mts (44) and Qionglai Mts (45) (Supplementary Fig. 1). These areas contain not only the highest plant diversity and endemism, but are also recognized as evolutionary cradles in China (r ∈ (0.67, 0.90), Fig. 3d–f)[28,29]. There are two potential explanations for the above pattern. (1) The evolution of traits associated with extinction risks (e.g., morphology, habitat type, and chemical composition) each follows a degree of non-random evolutionary trajectories, and taxa with these traits are usually phylogenetically related and more likely to adapt to similar environmental and climatic conditions[6,30]. (2) Geological history theories generally assume that the spatial distribution of a species and its concordant

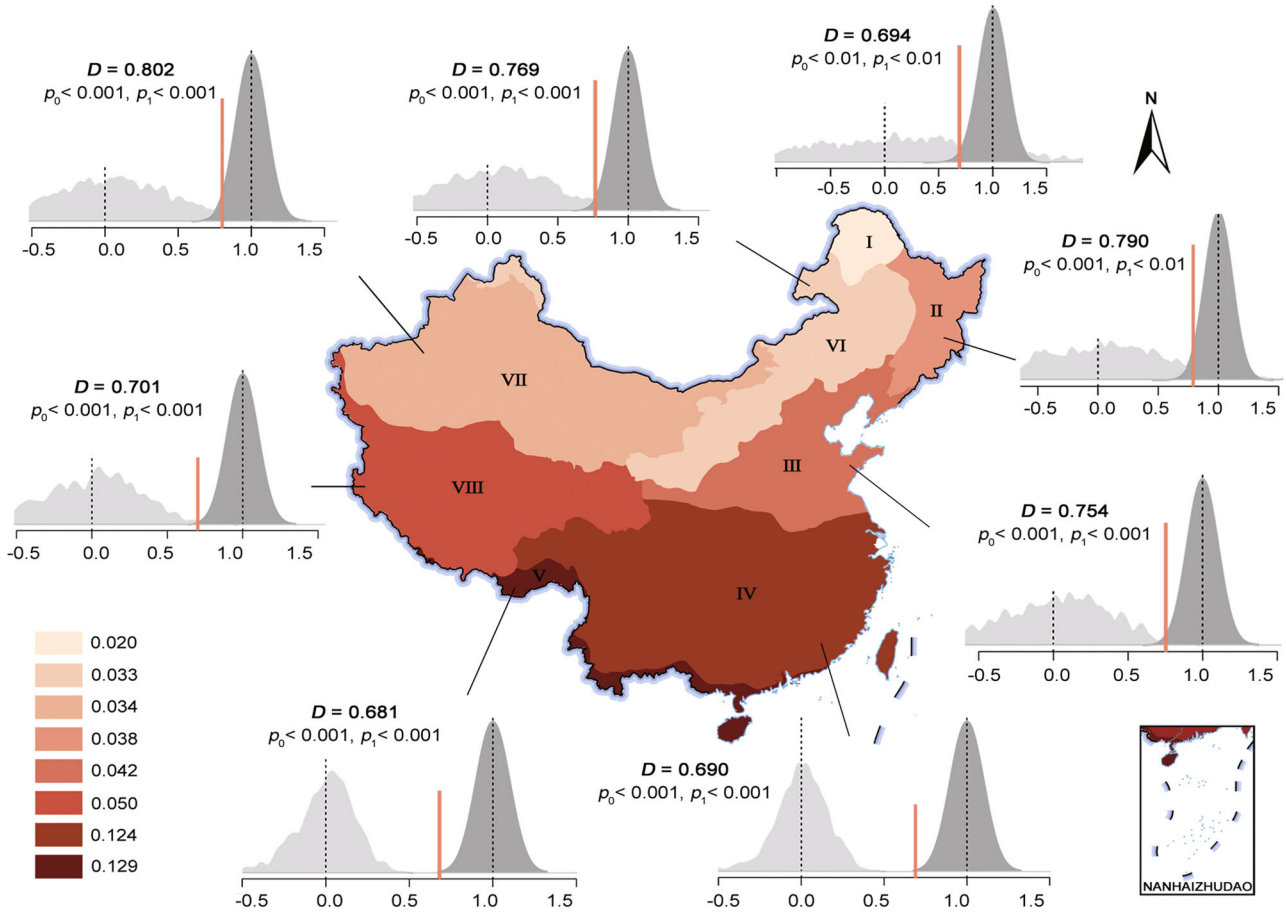

Fig. 4 | Proportions and phylogenetic signals of threatened species in different vegetation regions of China. The names of vegetation regions are shown in Fig. 2 and the background color represents the proportion of threatened species (dividing threatened species richness by total species richness) for each vegetation region. The simulated diagrams of phylogenetic signals of threatened species for eight vegetation regions are shown around the map, with the distribution of *D* values assumed to be a Brownian motion (gray) and a random model (dark gray), respectively. The red solid lines show the observed *D* values. p_0 and p_1 are *p*-values significantly different from the Brownian motion ($D = 0$; the dotted line) or random model ($D = 1$; the dotted line) expectation, respectively. The national boundary layer was downloaded from the Standard Map Service Website (Approval Number is GS(2019)1823; http://bzdt.ch.mnr.gov.cn/browse.html?picId=%224o28b0625501ad13015501ad2bfc0256%22, accessed October 2022).

extinction risk in southwest mountainous areas of China are mainly shaped by topographic heterogeneity[9]. Topographic heterogeneity within these areas has led to the formation of a variety of small, complex ecological climate and related dispersal barriers, which might have influenced gene exchange between populations and species[31]. When a suitable external environment appears, localized species may diverge and radiate rapidly. But species that evolve in this manner are usually specifically adapted to local environments, and most of them are naturally vulnerable to even small environmental disturbances[5,9,25]. Therefore, during the evolutionary process of speciation, the conservatism of specific intrinsic traits and a species' strict requirements for complex ecological environments may both drive a concentration of species within specific ranges of latitude, longitude, and elevation[32,33]. These long-term aggregation processes continuously contribute to both the concentration of threatened flowering plants and their phylogenetic endemism.

We find that spatial extinction risks of flowering plants in China are driven by multiple potential drivers and are also extent dependent. At the national level, vegetation structures, represented by the proportions of herbs (R_herb) or trees (R_tree), are the direct dominant drivers of extinction risk, followed by climatic drivers (i.e., precipitation, Prec) and evolutionary drivers (i.e., median divergence time, medianDT) (Supplementary Figs. 3–5). While extinction drivers vary across vegetation regions, a clear geographical continuity can be observed with some adjacent regions sharing similar dominant drivers (Fig. 6). Moreover, such geographical continuity in extinction drivers has been confirmed by patterns of the zone-level analyses, with West China dominated by vegetation structure drivers, South China by climatic drivers, and North China by evolutionary drivers (Fig. 5; Supplementary Data 15).

In West China, vegetation structure represents the strongest extinction threat of many localized plant species. The proportion of herbs in this region is significantly higher than trees and shrubs (Supplementary Fig. 6), probably resulting in an imbalance in "tree-shrub-herb" ecotypes and compositional instability in most local communities, but also reflecting the adaptive potential for herbs to speciate in such environments[34]. These ecologically fragile ecosystems, coupled with extreme habitats, might have led to a decline in phylogenetic diversity and possibly functional diversity of local communities. In such circumstances, localized adaptation may optimize reproductive strategies while simultaneously increasing long-term extinction risk in these harsh environments. For instance, *Saussurea*, a genus of the family Asteraceae with a diversity center in *Qinghai-Tibet Plateau alpine vegetations*, maximizes resource allocation to seed production to enhance reproductive output and therefore evolutionary longevity[35]. However, the extremely fragile vegetation composition, dramatically changeable temperature, and long seasonal drought in West China, may make these 'trade-offs' in survival strategy

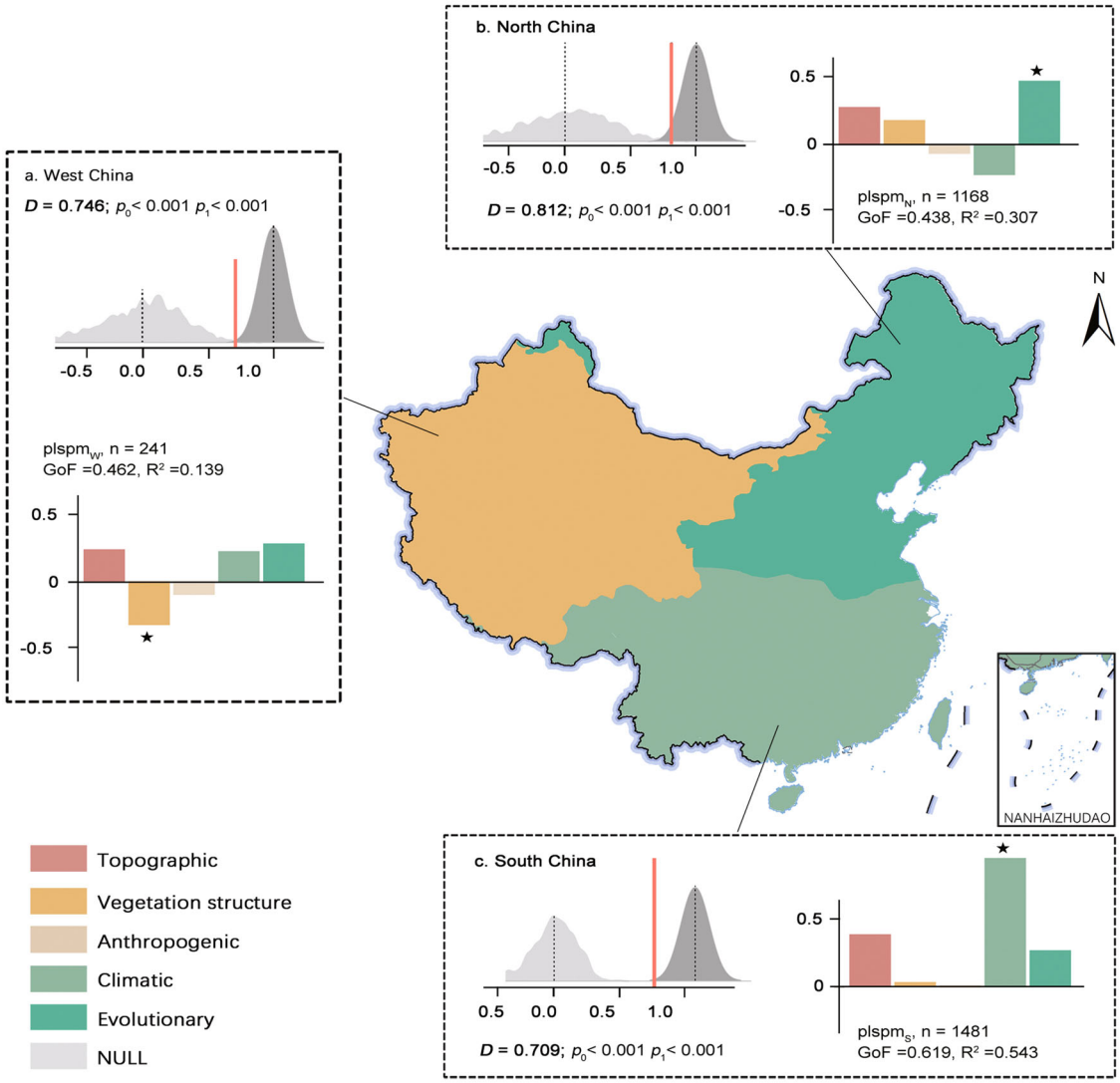

Fig. 5 | Phylogenetic signals, spatial threatening processes and potential extinction drivers for flowering plants in different zones based on *zone-plspms*. The map shows the spatial patterns of dominant drivers in three zones under the total effects of *zone-plspms*. The simulated diagrams of phylogenetic signals of threatened flowering plants for three zones are shown around the map (**a**–**c**), with the distribution of *D* values assumed to be a Brownian motion (gray) and a random model (dark gray), respectively. Barchars in boxes (**a**–**c**) show the total effects of five types of potential extinction drivers. Model name ($plspm_W$, $plspm_N$, and $plspm_S$), sample size (n), value of goodness of fit (GoF), and explanatory power of threatened species (R^2) for each zone are shown near the barcharts. The national boundary layer was downloaded from the Standard Map Service Website (Approval Number is GS(2019)1823; http://bzdt.ch.mnr.gov.cn/browse.html?picId=%224o28b0625501ad13015501ad2bfc0256%22, accessed October 2022).

for herbaceous flowering plants only alleviate, rather than prevent, their tendency toward extinction.

In the humid regions of South China, climatic drivers dominate the high-risk extinction of local flowering plants. The extinction risks increase with greater annual total precipitation (Prec) and average annual optimal temperature (Topti) (Supplementary Data 14). Mountainous areas (e.g., *Subtropical evergreen broad-leaved forests*) tend to form microclimates and unique habitats that constrain population migration and gene flow, leading to unstable populations and loss of genetic variation[9,36]. Furthermore, persistent global warming and increasing anthropogenic pressures are driving an upward migration and even local extinction of montane flowering plants[9,37].

Another important finding is that evolutionary drivers dominate the high-risk extinction of flowering plants in North China. The flora of this region has a unique and ancient evolutionary history[29] and the Changbai Mountain range has been recognized as a center of paleo-endemism[28]. The extinction risk of flowering plants in this region is primarily influenced by their divergence time, diversification rate, and weighted evolutionary distinctiveness. We find numerous relict plants in this region that belong to isolated lineages in the phylogenetic tree and are at high risk of extinction, including *Schisandra chinensis*, *Caldesia parnassifolia*, and *Asarum sieboldii*, indicating the high weighted evolutionary distinctiveness of this region. Our finding suggests that evolutionary drivers have played a significant role in promoting the spatial extinction risks of flowering plants in North China, which have been largely overlooked in previous studies[24,25,38,39].

Moreover, due to the intricate nature of extinction risks and extent effect of extinction drivers, partition analyses at different levels are necessary to accurately comprehend the characteristics of individual drivers. For instance, the effects of anthropogenic drivers are almost all insignificant in the *national-plspm* (Supplementary Data 6) and *zone-plspm* (Supplementary Data 15), but are variably significant in specific vegetation regions based on *regional-plspm*s (i.e., VIII; Supplementary Data 11). This indicates that elucidating the spatial

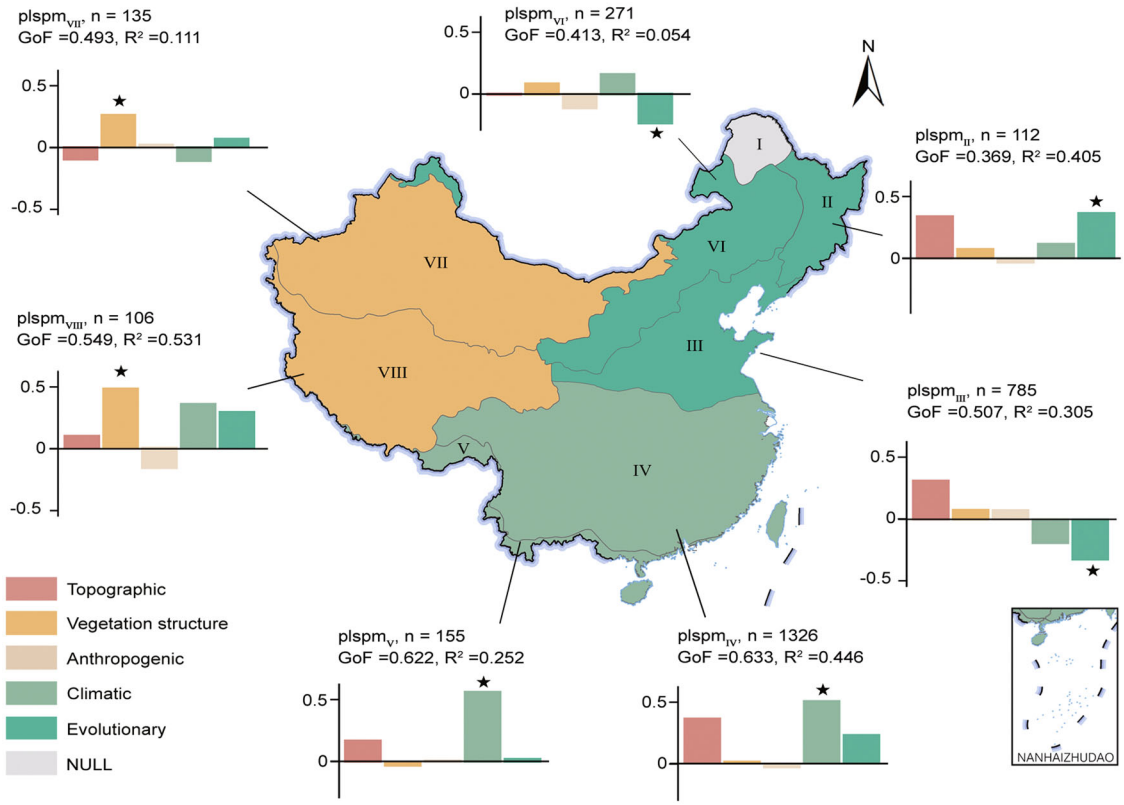

Fig. 6 | Spatial threatening processes and potential extinction drivers of flowering plants in different vegetation regions based on *regional-plspms*. The map shows the spatial patterns of dominant driver for each vegetation region under the total effects of *regional-plspms*. Barchars with different colors show the total effects of five types of drivers for vegetation regions II, III, IV, V, VI, VII, and VIII, respectively. The black stars show the dominant driver for each region. Model name (plspm$_{II}$–plspm$_{VIII}$), sample size (n), value of goodness of fit (GoF), and explanatory power of threatened species (R^2) for each vegetation region are shown above the barcharts. The national boundary layer was downloaded from the Standard Map Service Website (Approval Number is GS(2019)1823; http://bzdt.ch.mnr.gov.cn/browse.html?picId=%224o28b0625501ad13015501ad2bfc0256%22, accessed October 2022).

threatened processes by treating large-extent areas as a single region cannot accurately unravel the actual state of biodiversity with highly heterogeneous extinction risks. Therefore, it is essential to divide a large area into smaller regions or zones with significant internal consistency and external disparities in vegetation characteristics.

Understanding the spatial variability of extinction risk and its underlying drivers is crucial for predicting future range shifts and extinction tendencies for extant biodiversity. In particular, identification of the spatial heterogeneity of extinction risk across different spatial extents can inform targeted and cohesive conservation and recovery strategies. Protected areas that conserve vulnerable species and significant evolutionary lineages in China should be created in a timely manner according to these spatial characteristics of extinction risk.

In the sparsely populated region of West China, extinction risk of biodiversity is dominated by vegetation structure drivers and establishing large-scale protected areas is considered appropriate. In addition to protecting ecosystem integrity and community stability, large-scale protected areas can provide windows of time and space for ecological restoration of fragile and degraded habitats. In North China, which is home to many highly evolutionarily distinct species, high-risk extinction of flowering plants is driven mainly by evolutionary drivers. To mitigate the irreversible loss of evolutionarily ancient and distinct lineages facing unpredictable extinctions, we recommend establishment of comprehensive protected areas. Much of South China is characterized by highly heterogeneous climate and topography[22,37], including localized regions with high species diversity, threatened species diversity, species endemism, and phylogenetic diversity (Figs. 2, 3 and Supplementary Figs. 1, 7)[28,29]. Here, protection networks connected by ecological corridors should be established to promote migration among populations of species. This approach would not only preserve current living conditions of more than 80% of the Chinese human population[40] but also facilitate in situ protection as much as possible.

The strong spatial heterogeneity of threatening processes on flowering plants in China calls for the development of varying conservation strategies according to the dominant threatening factors within each region. Understanding the spatial characteristics of extinction risk, and their underlying drivers, is critical to developing multidimensional conservation strategies that can link biodiversity loss and risks to the attainment of sustainable development[41].

Methods

Phylogeny and extinction risk

The phylogeny used in this study was based on an existing species-level tree of life of flowering plants in China[29]. The original phylogeny was reconstructed by Hu et al. [42], which included 13,321 species (12,160 native to China) and 2991 genera (2743 native to China). The phylogeny was dated by Lu et al. [29]. with 138 calibrations, using the penalized likelihood (PL) approach as implemented in treePL[43]. Complete species trees were then generated by inserting 13,864 additional species without sequence data into the randomly selected nodes below the corresponding genera of the backbone tree with the "V.PhyloMaker"[44] package in R[45], according to available taxonomic information. Finally, a set of complete species trees that include 27,185 species representing 2859 genera from 252 families of

flowering plants native to China were generated. In this study, we selected the first complete species tree in 10_species_trees_27,185sp_s2.tre (https://doi.org/10.5061/dryad.6m905qg2w) for downstream analyses.

The IUCN Red List Categories and Criteria represent an easily and widely understood system for evaluating the threatened status of species[46]. We herein quantified the extinction risk of flowering plants in China according to the Red List of Higher Plants of China (https://www.mee.gov.cn/xxgk2018/xxgk/xxgk01/202305/t20230522_1030745.html)[19]. Species were classified as Extinct (EX), Extinct in the wild (EW), Regional extinct (RE), Critically endangered (CR), Endangered (EN), Vulnerable (VU), Near threatened (NT), Least concern (LC) and Data deficient (DD)[46]. Species ranked as CR, EN, and VU were considered threatened species (i.e., high-risk flowering plants in this study), which represent about 9.8% (2659 species) of the total flowering plants of China.

Distribution records

Species distribution records were obtained from two primary sources, i.e., literature and public databases. About 1.69 million county-level distribution records were obtained from *Flora Republicae Popularis Sinicae* (FRPS, http://www.iplant.cn/frps, accessed October, 2022), *Flora of China* (FOC, http://www.efloras.org/flora_page.aspx?flora_id=2, accessed October, 2022) and available regional floras (Supplementary Data 16). An additional 6.85 million collection records were obtained from the Chinese Virtual Herbarium (CVH, https://www.cvh.ac.cn/, accessed October, 2022) and the Global Biodiversity Information Facility (GBIF, https://www.gbif.org/[47], accessed January, 2021). After removing invalid and duplicate records and and outliers, about 0.84 million county-level distribution records were retained in the specimen database.

We combined the literature database with the specimen database to form a comprehensive distribution database and followed the flowchart in Supplementary Fig. 8 to process the distribution records. We (1) standardized the taxonomic names of distribution records according to the checklist of native flowering plants of FOC; (2) standardized the county names of records according to codes available at http://www.mca.gov.cn/ (total number of counties: 2894); (3) combined the distribution records of infraspecific taxa into corresponding species; and (4) removed duplicate records to ensure that only one distribution record per species per county was retained. Ultimately, 2.02 million county-level distribution records were retained for further analyses. It should be noted that in addition to man-made and historical influences, the division of administrative counties in China is also closely related to environmental factors such as topography, geomorphology, and climate.

Measures of spatial diversity patterns

We defined the species diversity of flowering plants, endemic flowering plants, and threatened flowering plants in each county as species richness (SR), endemic species richness (ER), and threatened species richness (TR) for each county, respectively. The proportion of threatened species (propTR) for each county was calculated by dividing TR by SR in each county. Faith's phylogenetic diversity (PD), defined as the total branch length spanned by the tree including all species in a local community[48], was used to estimate the evolutioanry history of flowering plants in each county. We calculated the standardized effective size of PD (sesPD) using "Picante"[49] package in R[45] to test the phylogenetic relatedness of threatened species within counties. We generated null distributions of PD for each county by shuffling taxa labels 999 times while threatened species occurrence frequency and sampled species richness remained constant. We compared the observed PD to the mean of the null distribution by calculating a standardized effective size (sesPD) using the values of (PD-mean(null))/SD(null). Negative values of sesPD indicate phylogenetic clustering (i.e., threatened species are more closely related than expected), whereas positive values indicate phylogenetic overdispersion (i.e., threatened species are less closely related than expected). We also followed the method of Rosauer et al. to calculate phylogenetic endemism (PE) for each county by summing the valuses of PD/distribution range of a clade[50].

Extinction drivers

According to the hypotheses outlined in Fig. 1 and Supplementary Data 1, the potential extinction drivers for flowering plants in China were calculated below.

Evolutionary drivers. Divergence time (DT) is the time since a species divided from its closest sister group[7]. We used the median divergence time (medianDT) of flowering plants in a county to measure its divergence time. Divergence time for each species was extracted from a dated phylogeny of flowering plants in China, as previous studies have revealed that it is reasonable to compare divergence times from taxon-rich regional phylogenies within regions and in a relative manner[51]. We used diversification rate (DR) of the terminal species, i.e., representing present-day species, to describe the geographic patterns of diversity[52–54]. We followed Jetz et al.'s method to measure the species-level lineage diversification rate (DR) for each species based on the equal-splits metric[53]. Specifically, it was calculated as the number of nodes that separate each species from the root of the tree weighted by the length of the branch, i.e., the distance of each node to the present[53]. We also defined the median diversification rate of terminal species within a county (medianDR) to measure the diversification rate of the county according to Jetz et al. [53]. Evolutionary distinctiveness (ED) of a species was calculated by dividing the total PD of a clade among its members. This method can measure how isolated a species is on the phylogenetic tree[55].

To obtain the weighted evolutionary distinctiveness (WED) of each species, we calculated the accumulated area of each species by dividing its area of distribution into different altitude belts at 300 meter intervals and removed unoccupied belts according to the actual altitudinal distribution of each species (Supplementary Note 2 and Supplementary Data 17). We then constrained the accumulated area of the remaining belts of each species to be its suitable geographic range size. WED (Ma/10,000 km2) refers to its ED divided by its total geographic range size[54]. Median weighted evolutionary distinctiveness (medianWED) of all flowering plants within a county was used to represent each county's WED in our analyses. We calculated PE and ED in the packages of "canaper"[56] and "Caper"[57] in R[45], respectively.

Vegetation structure drivers. In this study, all potential drivers applying to localized flowering plants that are caused by narrow ecological factors, including vegetation composition and types, are collectively referred to as vegetation structure drivers (Supplementary Data 1). We followed previous large-scale studies to define the proportions of species with different growth forms in a county to quantify regional vegetation structure[58]. We extracted the proportions of herbs (R_herb), trees (R_tree) and shrubs (R_shrub) of all flowering plants in each county from the datasets of Qin[59] and Chen et al. [60]. To avoid bias caused by incomplete sampling, the relative proportions of lianas, aquatic and epiphytic plants were not considered.

To further clarify the drivers of different vegetation structures on the extinction risks for flowering plants in China, we extracted vegetation types (vegType) and vegetation groups (vegGroup) for each county according to the *1:1,000,000 Chinese Vegetation Atlas*[61], which has divided China's vegetation communities into 58 types (Supplementary Fig. 9a) and 11 groups by merging similar vegetation types (Supplementary Fig. 9b). We also merged adjacent patches of the same vegetation type together in the layer of *1:1,000,000 Chinese Vegetation Atlas* to ensure that patches of the same vegetation type are not

adjacent within a county[61]. We then defined the number of vegetation patches in the county as the degree of vegetation fragmentation (vegFrag) to quantify the fragmentation of environments facing biodiversity loss.

Climatic drivers. The datasets of average annual minimum temperature (°C), average annual maximum temperature (°C) and average annual total precipitation (mm) from the Climatic Research Unit (GRU-TS 4.03) on the platform of WorldClim 2.1 for nine years (2010–2018) were selected to quantify the impact of climate on spatial threatening processes of flowering plants[62,63]. Based on the three datasets described above, we first calculated annual minimum temperature (Tmin), annual maximum temperature (Tmax) and annual total precipitation (Prec) for each county, respectively. Then we defined half of the sum of Tmin and Tmax and the difference between Tmin and Tmax as the average annual optimal temperature (Topti) and the range of different temperatures (Trang) for flowering plants in each county, respectively. Finally, we extracted the average temperature vegetation dryness index (TVDI) from all pixels in each county to quantify the impact of drought on extinction risks of flowering plants (see Supplementary Data 2, Supplementary Note 2 and Supplementary Fig. 10).

Topographic drivers. Topographic drivers in this study mainly include topography and spatial location (Supplementary Data 1). We identified several potential topographic drivers based on SRTM30 digital elevation model (DEM, version 2, https://www2.jpl.nasa.gov/srtm/). We defined the average elevation (avgElev) of all sampling points in each county as the county's elevation and the difference between the maximum elevation (maxElev) and the minimum elevation (minElev) as the county's elevation variation (variElev) (Supplementary Note 2). The degree of surface roughness in a county was defined as topographic roughness (topoRough) (Supplementary Fig. 11). We also used the longitude (Long) and latitude (Lat) of the geometric center of each county to represent the spatial locality of each species within that county.

Anthropogenic driver. In this study, the global human footprint was selected to measure direct impact of anthropogenic effects on flowering plants of China (Supplementary Data 1 and Supplementary Fig. 12)[64]. The county-level human footprint (HFP) was extracted from the global human footprint database (https://doi.org/10.5061/dryad.052q5) according to the county-level boundaries.

Phylogenetic signals

Fritz's *D* statistic was used to measure phylogenetic signals of extinction risks for flowering plants in China (threatened were marked with 1 and otherwise with 0)[65,66] among vegetation regions and zones, respectively. We used phylo.D function in R package "caper"[57] to calculate Fritz's *D* value, which compares the sum of changes in estimated nodal values of a binary trait (threatened or not) along branches of the phylogeny against the random and Brownian expectations. $D = 1$ suggests that the trait (threatened or not) has evolved randomly with respect to the phylogeny, and $D > 1$ suggests that the trait is more overdispersed than the random expectation. $D = 0$ indicates that the trait has evolved following the Brownian model, and $D < 0$ indicates that the trait is more phylogenetically conserved than the Brownian expectation. $D \in (0, 1)$ indicates a gradient of possible scenarios between pure Brownian and pure random evolution[65]. Two *p*-values are further calculated based on the simulations with 999 permutations, where p_1 ($D < 1$) and p_0 ($D > 0$) respectively indicate the probability of the *D* value of the binary trait resulting from a random or Brownian phylogenetic structure. We reported the exact values of Fritz's *D* statistic directly, as categorizing the strength of a phylogenetic signal as strong, moderate, or weak is considered subjective and contentious[66].

Spatial analyses

To test whether the spatial extinction risks of flowering plants within the same region are more similar than those among regions, we used the *q* statistic to quantify the degree and significance of spatial heterogeneity for different diversity measures. The value of *q* ranges from −1 to 1; the larger the *q* is, the more significant the spatial heterogeneity is[67].

To reduce the inconvenience and bias caused by numerous factors, we used two analyses to filter extra factors in the modeling. The modified *t*-test in the "SpatialPack" package of R[68] was used to check the spatial consistency between diversity measures (i.e., TR and propTR) and potential extinction drivers (*r*). The value of *r*, ranges from −1 to 1, was used to quantify the degree of spatial consistency; and the larger the *r* is, the higher the spatial consistency of biodiversity measures is[68]. The Moran's *I* was used to examine the spatial autocorrelation of diversity measures (i.e., TR and propTR) and potential extinction drivers, respectively. The value of *I* ranges from −1 to 1. The closer *I* is to 1 (high z-scores and appropriate *p* value), the more clustered the spatial distribution of a diversity measure is; the closer *I* is to −1, the more discrete the measure is; the closer *I* is to 0, the more random the measure is[27].

Spatial modeling

Plspm (partial least squares path model) has been widely used to assess complicated environmental impacts in studies such as species richness, ecological environment, agri-tourism and sustainability[69–71]. In this study, plspm was used to investigate how biodiversity-intrinsic and -extrinsic factors have contributed to the spatial extinction risks of flowering plants (propTR) in China at varying spatial extents. The latent variables in our plspms here included evolution, climate, topography, vegetation and anthropogenic effects. Generally, the nested phylogenetic relationships between clades should be taken into consideration in models that treated extinction risks of evolutionary clades as the response variables. However, in our spatial threatened modeling, the response variables were the extinction risks of flowering plants of different geographic units, rather than extinction risks of different evolutionary clades. Nested phylogenetic relationships between clades were taken into a consideration when we quantified potential evolutionary drivers (i.e., medianDT, medianDR, and medianWED). The values of these evolutionary drivers with nested phylogenetic relationships of each geographic unit was calculated and mapped into corresponding units in each layer as a type of spatial driver prior to modeling. Therefore, it was not necessary to consider the nested phylogenetic relationships of clades again in the modeling. This spatial mapping method of evolutionary properties has been applied in many biodiversity conservation studies[12,54].

Several steps are necessary in spatial modeling (Supplementary Data 7). *Variable detection*. If the potential driver has an important influence on a diversity measure, the spatial pattern should also be similar to this measure[27,67]. We identified potential drivers by Moran's *I* of spatial autocorrelation and removed the randomly distributed drivers. *Variable standardization and null value processing*. All potential drivers (measured variables) were divided into five types: evolutionary, climatic, topographic, anthropogenic, and vegetation structure drivers (Fig. 1, Supplementary Fig. 13, and Supplementary Dataset 1, 3). Null values of some original layers were estimated by the random forest prediction method provided by the "MISSFOREST" package in R[72]. *Spatial model construction*. We designed a metamodel containing five types of extinction drivers (latent variables), whose inner model and outer model consisted of the latent variables and extinction risk (such as TR) and the latent variables and their relevant specific factors, respectively (Supplementary Fig. 13). In plspm, each latent variable could include one or more manifest variables. The path coefficients represented the directions and strength of relationships among latent variables, and the explained variability (R2) was also estimated.

To explore potential drivers of extinction risk for flowering plants in China, a region with high climatic and topographic heterogeneity, and to elucidate the extent-dependent characteristics of extinction risk, we constructed three sets of models tailored to different spatial extents: *national-plspm* for the whole of China, *regional-plspm*s for the vegetation regions, and *zone-plspms* for zones. We first constructed a *national-plspm* to explain the spatial extinction risk (propTR, hereafter) affecting all flowering plants in China based on the metamodel (Supplementary Fig. 13). Due to the significant heterogeneity of extinction risk for flowering plants, we then divided China into eight distinct regions (Fig. 2) based on the *Vegetation Regionalization Map of China (1: 6,000,000)* (from Resources and Environmental Sciences and Data Center, http://www.resdc.cn/, accessed October, 2022). We then constructed eight *regional-plspm*s to explain the spatial extinction risks of flowering plants for each vegetation region (Supplementary Data 2). The $plspm_{II}$, $plspm_{III}$, $plspm_{IV}$, $plspm_{V}$, $plspm_{VI}$, $plspm_{VII}$, and $plspm_{VIII}$ were names of models for the eight vegetation regions. The model for *Cold temperate coniferous forests* ($plspm_{I}$) cannot be implemented because it does not meet the requirement of a minimum sample size (>30). We further constructed three *zone-plspms* by dividing China into three zones, West China, North China, and South China, according to precipitation, climate types and incorporating vegetation boundaries, to further test whether spatial extinction risks of flowering plants in China are extent-dependent. The $plspm_{W}$, $plspm_{N}$, and $plspm_{S}$ were names of models for three zones, i.e., West China, North China, and South China, respectively.

We then evaluated the reliability of all models by verifying the one-dimensionality of latent variables, the validity of inner and outer models, and the significance of path coefficients (representing the direction and strength of relationships between latent variables) of different models based on a bootstrap resampling. Lastly, we continuously optimized these models until these parameters meet the requirements (Supplementary Note 3 and Supplementary Data 7). The construction and verification of each model was conducted using the "plspm" package in R (9999 bootstraps)[73].

Reporting summary

Further information on research design is available in the Nature Portfolio Reporting Summary linked to this article.

Data availability

All original data used in this study are available from published literature or publicly available databases. The Methods and Supplementary file include all original data sources, citations, web-links, and detailed descriptions of input variables. The dated phylogenies of flowering plants in China were published in Lu et al.[29]. and are available in Dryad (https://doi.org/10.5061/dryad.6m905qg2w). Map-based distribution data are available in ScienceDB (https://www.scidb.cn/en/s/J3mUry). The data generated in this study are provided in the Supplementary Information/Source Data file. Source data for the simulated diagrams of phylogenetic signals in Figs. 4 and 5 can be found in ScienceDB (https://www.scidb.cn/en/detail?dataSetId=c1b2235310914c4a9ba65864c40fe1bf)[74]. Source data are provided with this paper.

Code availability

The code used in this article are available in the following repository: https://www.scidb.cn/en/detail?dataSetId=c1b2235310914c4a9ba65864c40fe1bf[74].

References

1. Mace, G. M. et al. Aiming higher to bend the curve of biodiversity loss. *Nat. Sustain.* **1**, 448–451 (2018).
2. Hull, P. M., Darroch, S. A. & Erwin, D. H. Rarity in mass extinctions and the future of ecosystems. *Nature* **528**, 345–551 (2015).
3. Humphreys, A. M., Govaerts, R., Ficinski, S. Z., Nic Lughadha, E. & Vorontsova, M. S. Global dataset shows geography and life form predict modern plant extinction and rediscovery. *Nat. Ecol. Evol.* **3**, 1043–1047 (2019).
4. Vamosi, J. C. & Wilson, J. R. U. Nonrandom extinction leads to elevated loss of angiosperm evolutionary history. *Ecol. Lett.* **11**, 1047–1053 (2008).
5. Li, J. et al. Taxonomic and geographic selectivity of spermatophytes' extinction risk in China. *Biodivers. Conserv.* **273**, 109669 (2022).
6. Roy, B. K., Hunt, G. & Jablonski, D. Phylogenetic conservatism of extinctions in marine bivalves. *Science* **325**, 731–737 (2009).
7. Verde Arregoitia, L. D., Blomberg, S. P. & Fisher, D. O. Phylogenetic correlates of extinction risk in mammals: species in older lineages are not at greater risk. *Proc. R. Soc. B* **280**, 1–7 (2013).
8. Harfoot, M. B. J. et al. Using the IUCN Red List to map threats to terrestrial vertebrates at global scale. *Nat. Ecol. Evol.* **5**, 1510–1519 (2021).
9. Jensen, D. A., Ma, K. & Svenning, J. C. Steep topography buffers threatened gymnosperm species against anthropogenic pressures in China. *Ecol. Evol.* **10**, 1838–1855 (2020).
10. Shrestha, N., Xu, X., Meng, J. & Wang, Z. Vulnerabilities of protected lands in the face of climate and human footprint changes. *Nat. Commun.* **12**, 1632 (2021).
11. Kubota, Y., Kusumoto, B., Shiono, T., Ulrich, W. & Duarte, L. Environmental filters shaping angiosperm tree assembly along climatic and geographic gradients. *J. Veg. Sci.* **29**, 607–618 (2018).
12. Dinnage, R., Skeels, A. & Cardillo, M. Spatiophylogenetic modelling of extinction risk reveals evolutionary distinctiveness and brief flowering period as threats in a hotspot plant genus. *Proc. R. Soc. B* **287**, 20192817 (2020).
13. Greenberg, D. A. et al. Evolutionary legacies in contemporary tetrapod imperilment. *Ecol. Lett.* **24**, 2464–2476 (2021).
14. Molina-Venegas, R., Ramos-Gutiérrez, I. & Moreno-Saiz, J. C. Phylogenetic patterns of extinction risk in the endemic flora of a mediterranean hotspot as a guiding tool for preemptive conservation actions. *Front. Ecol. Evol.* **8**, 571587 (2020).
15. Yessoufou, K., Daru, B. H. & Davies, T. J. Phylogenetic patterns of extinction risk in the eastern arc ecosystems, an African biodiversity hotspot. *PLoS ONE* **7**, e47082 (2012).
16. Tye, M., Dahlgren, J. P., Øien, D.-I., Moen, A. & Sletvold, N. Demographic responses to climate variation depend on spatial - and life history -differentiation at multiple scales. *Biodivers. Conserv.* **228**, 62–69 (2018).
17. Liang, M. et al. Consistent stabilizing effects of plant diversity across spatial scales and climatic gradients. *Nat. Ecol. Evol.* **6**, 1669–1675 (2022).
18. Qin, H. & Zhao, L. Evaluating the threat status of higher plants in China. *Biodivers. Sci.* **25**, 689–695 (2017).
19. Qin, H. et al. Threatened species list of China's higher plants. *Biodivers. Sci.* **25**, 696–744 (2017).
20. Li, L. et al. Red list assessments of Chinese higher plants. *Int. J. Digit. Earth* **16**, 2762–2775 (2023).
21. Mi, X. et al. The global significance of biodiversity science in China: an overview. *Natl. Sci. Rev.* **8**, nwab032 (2021).
22. Xia, C. et al. Developing long-term conservation priority planning for medicinal plants in China by combining conservation status with diversity hotspot analyses and climate change prediction. *BMC Biol.* **20**, 89 (2022).
23. Xu, W. et al. Human activities have opposing effects on distributions of narrow-ranged and widespread plant species in China. *Proc. Natl. Acad. Sci. USA* **116**, 26674–26681 (2019).
24. Lu, Y. et al. Spatial variation in biodiversity loss across China under multiple environmental stressors. *Sci. Adv.* **6**, eabd0952 (2020).

25. Yu, H., Sui, X., Sun, M., Yin, X. & Deane, D. C. Relative importance of ecological, evolutionary and anthropogenic pressures on extinction Risk in Chinese angiosperm genera. *Front. Ecol. Evol.* **10**, 844509 (2022).
26. Chen, Y. et al. Extinction risk of Chinese angiosperms varies between woody and herbaceous species. *Divers. Distrib.* **29**, 232–243 (2022).
27. Li, H., Calder, C. A. & Cressie, N. Beyond Moran's *I*: testing for spatial dependence based on the spatial autoregressive model. *Geogr. Anal.* **39**, 357–375 (2007).
28. Zhang, X. et al. Spatial phylogenetics of the Chinese angiosperm flora provides insights into endemism and conservation. *J. Integr. Plant Biol.* **64**, 105–117 (2022).
29. Lu, L. et al. A comprehensive evaluation of flowering plant diversity and conservation priority for national park planning in China. *Fundam. Res.* **3**, 939–950 (2023).
30. Zacaï, A. et al. Phylogenetic conservatism of species range size is the combined outcome of phylogeny and environmental stability. *J. Biogeogr.* **44**, 2451–2462 (2017).
31. Yu, J. et al. Integrated phylogenomic analyses unveil reticulate evolution in *Parthenocissus* (Vitaceae), highlighting speciation dynamics in the Himalayan-Hengduan Mountains. *New Phytol.* **238**, 888–903 (2023).
32. Davies, T. J. et al. Extinction risk and diversification are linked in a plant biodiversity hotspot. *PLoS Biol.* **9**, e1000620 (2011).
33. Tanentzap, A. J., Igea, J., Johnston, M. G. & Larcombe, M. J. Does evolutionary history correlate with contemporary extinction risk by influencing range size dynamics? *Am. Nat.* **195**, 569–576 (2020).
34. Friedman, J. The evolution of annual and perennial plant life histories: ecological correlates and genetic mechanisms. *Annu. Rev. Ecol. Evol. Syst.* **51**, 461–481 (2020).
35. Zhang, X. et al. Macroevolutionary pattern of *Saussurea* (Asteraceae) provides insights into the drivers of radiating diversification. *Proc. R. Soc. B* **288**, 20211575 (2021).
36. Lan, G., Hu, Y., Cao, M. & Zhu, H. Topography related spatial distribution of dominant tree species in a tropical seasonal rain forest in China. *For. Ecol. Manage.* **262**, 1507–1513 (2011).
37. Elsen, P. R., Monahan, W. B. & Merenlender, A. M. Topography and human pressure in mountain ranges alter expected species responses to climate change. *Nat. Commun.* **11**, 1974 (2020).
38. Qin, H. et al. Evaluating the endangerment status of China's angiosperms through the red list assessment. *Biodivers. Sci.* **25**, 745–757 (2017).
39. Wei, F., Nie, Y., Miao, H., Lu, H. & Hu, Y. Advancements of the researches on biodiversity loss mechanisms. *Chin. Sci. Bull. (Chin. Version)* **59**, 430 (2014).
40. Liu, T., Peng, R., Zhou, Y. & Cao, G. China's changing population distribution and influencing factors: Insights from the 2020 census data. *Acta Geogr. Sin.* **77**, 381–394 (2022).
41. Soto-Navarro, C. A. et al. Towards a multidimensional biodiversity index for national application. *Nat. Sustain.* **4**, 933–942 (2021).
42. Hu, H. et al. An updated Chinese vascular plant tree of life: Phylogenetic diversity hotspots revisited. *J. Syst. Evol.* **58**, 663–672 (2020).
43. Smith, S. A. & O'Meara, B. C. treePL: divergence time estimation using penalized likelihood for large phylogenies. *Bioinformatics* **28**, 2689–2690 (2012).
44. Jin, Y. & Qian, H. V.PhyloMaker: an R package that can generate very large phylogenies for vascular plants. *Ecography* **42**, 1–7 (2019).
45. R Core Team. *R: a language and environment for statistical computing*. (R Foundation for Statistical Computing, 2021).
46. IUCN. *IUCN Red list categories and criteria: version 3.1*. (IUCN Species Survival Commission, Gland, 2001).
47. GBIF.org. (22 January 2021) GBIF occurrence Download https://doi.org/10.15468/dl.bu72c5) (2021).
48. Faith, D. P. Conservation evaluation and phylogenetic diversity. *Biodivers. Conserv.* **61**, 1–10 (1992).
49. Kembel, S. W. et al. Picante: R tools for integrating phylogenies and ecology. *Bioinformatics* **26**, 1463–1464 (2010).
50. Rosauer, D., Laffan, S. W., Crisp, M. D., Donnellan, S. C. & Cook, L. G. Phylogenetic endemism: a new approach for identifying geographical concentrations of evolutionary history. *Mol. Ecol.* **18**, 4061–4072 (2009).
51. Molina-Venegas, R. & Lima, H. Should we be concerned about incomplete taxon sampling when assessing the evolutionary history of regional biotas? *J. Biogeogr.* **48**, 2387–2390 (2021).
52. Shrestha, N. et al. Global patterns of Rhododendron diversity: The role of evolutionary time and diversification rates. *Glob. Ecol. Biogeogr.* **27**, 913–924 (2018).
53. Jetz, W., Thomas, G. H., Joy, J. B., Hartmann, K. & Mooers, A. O. The global diversity of birds in space and time. *Nature* **491**, 444–448 (2012).
54. Jetz, W. et al. Global distribution and conservation of evolutionary distinctness in birds. *Curr. Biol.* **24**, 919–930 (2014).
55. Isaac, N. J., Turvey, S. T., Collen, B., Waterman, C. & Baillie, J. E. Mammals on the EDGE: conservation priorities based on threat and phylogeny. *PLoS ONE* **2**, e296 (2007).
56. Paradis, E. *Analysis of phylogenetics and evolution with R*. (Springer Science & Business Media, 2012).
57. Orme, D. The caper package: comparative analysis of phylogenetics and evolution in R. https://cran.r-project.org/web/packages/caper/vignettes/caper.pdf. (2013).
58. Taylor, A., Weigelt, P., Denelle, P., Cai, L. & Kreft, H. The contribution of plant life and growth forms to global gradients of vascular plant diversity. *New Phytol.* **240**, 1548–1560 (2023).
59. Qin, H. *Seed plants of China: checklist, uses and conservation status*. 4 Volumes (Hebei Science and Technology Publishing House, Shijiazhuang, 2020).
60. Chen, Y., Ma, X., Du, Y. & Feng, M. *The Chinese aquatic plants*. (Henan Science and Technology Press, Zhengzhou, 2012).
61. Editorial Committee of Chinese Vegetation Atlas Chinese Academy of Sciences. *1:1,000,000 Chinese Vegetation Atlas*. (Geological Publishing House, Beijing, 2007).
62. Harris, I., Jones, P. D., Osborn, T. J. & Lister, D. H. Updated high-resolution grids of monthly climatic observations - the CRU TS3.10 Dataset. *Int. J. Climatol.* **34**, 623–642 (2014).
63. Fick, S. E. & Hijmans, R. J. WorldClim 2: new 1-km spatial resolution climate surfaces for global land areas. *Int. J. Climatol.* **37**, 4302–4315 (2017).
64. Venter, O. et al. Global terrestrial Human Footprint maps for 1993 and 2009. *Sci. Data* **3**, 160067 (2016).
65. Fritz, S. A. & Purvis, A. Selectivity in mammalian extinction risk and threat types: a new measure of phylogenetic signal strength in binary traits. *Conserv. Biol.* **24**, 1042–1051 (2010).
66. Molina-Venegas, R. How to get the most out of phylogenetic imputation without abusing it. *Methods Ecol. Evol.* **15**, 456–463 (2024).
67. Wang, J., Zhang, T. & Fu, B. A measure of spatial stratified heterogeneity. *Ecol. Indic.* **67**, 250–256 (2016).
68. Vallejos, R., Osorio, F. & Bevilacqua, M. in *Spatial relationships between two georeferenced variables: with applications in R* (Springer International Publishing, 2020).
69. Harris, G. & Pimm, S. L. Range size and extinction risk in forest birds. *Conserv. Biol.* **22**, 163–171 (2008).
70. Yang, H. et al. An integrated insight into the relationship between soil microbial community and tobacco bacterial wilt disease. *Front. Microbiol.* **8**, 2179 (2017).
71. Zhang, L. et al. Distinct methanotrophic communities exist in habitats with different soil water contents. *Soil Biol. Biochem.* **132**, 143–152 (2019).

72. Stekhoven, D. J. & Buhlmann, P. MissForest -non -parametric missing value imputation for mixed-type data. *Bioinformatics* **28**, 112–118 (2012).
73. Sanchez, G. *PLS path modeling with R*. (http://www.gastonsanchez.com. CA: Trowchez Editions, Berkeley, 2013).
74. Zhao. L., et al. Spatial heterogeneity of extinction risk for flowering plants in China. *Science Data Bank*. https://doi.org/10.57760/sciencedb.17283 (2024).

Acknowledgements

We thank Deyuan Hong, Anming Lu, Xiaoquan Wang, Qingfeng Wang, Guangwan Hu, Haining Qin, and Daming Zhang for valuable suggestions on this study. We thank Dan Xie and Yiyi Chen for providing representative photos of vegetation regions, Danxiao Peng, Yuchang Yang, Zhangjian Shan, Yun Liu, Qiang Zhang, Ang Li, Chengling Wang, Duan Liu, Ni Fang, Haowei Guo, Rindra Manasoa Ranaivoson, and Wyckliffe Omondi Omollo for assistance with data collection. We are also grateful to Huiyuan Liu and Tianxiang Chen for data assembalage, and Xiaoting Xu, Yangjun Lai, Jian Zhang, Miao Sun, Qian Zhang, Yalei Feng, and Yajuan Cao for valuable comments on the earlier drafts of the manuscript. This work was supported by National Natural Science Foundation of China (32122009 to L.L.), National Key Research Development Program of China (2022YFF0802300 to L.L. and 2023YFF0805800 to Z.C.), International Partnership Program of CAS (151853KYSB20190027 to Z.C.), Youth Innovation Promotion Association CAS (2020080 to L.L.), and Sino-Africa Joint Research Center, CAS (SAJC202101 to Z.C.). R.L.B. acknowledges support from the CAS President's International Fellowship Initiative.

Author contributions

Z.C., L.L., and L.Z. designed the study. L.Z., H.H., and B.L. compiled the data. L.Z. and J.L conducted the analyses. L.Z., L.L., Z.C., and R.L.B. led the writing and revision. All authors contributed to and approved the final manuscript.

Competing interests

The authors declare no competing interests.

Additional information

Supplementary information The online version contains supplementary material available at https://doi.org/10.1038/s41467-024-50704-3.

Correspondence and requests for materials should be addressed to Limin Lu or Zhiduan Chen.

Peer review information *Nature Communications* thanks Liping Li, Alicia Mastretta-Yanes and the other, anonymous, reviewer(s) for their contribution to the peer review of this work. A peer review file is available.